JOURNAL OF PROPULSION AND POWER
Vol. 17, No. 4, July–August 2001

Hub Wall Rotation Influence on High-Speed Compressor Cascade Performance

A. Doukelis,* K. Mathioudakis,† and K. Papailiou‡
National Technical University of Athens, Athens 15773, Greece

The influence of the magnitude of the relative wall speed on the performance of an annular compressor cascade with hub clearance is examined. Five-hole probe measurements, conducted at the inlet and outlet of the cascade, are used to derive blade performance characteristics, in the form of loss and turning distributions. Characteristics are presented in the form of circumferentially mass-averaged profiles, whereas distributions on the exit plane provide information useful to interpret the performance of the blading. Four different rotational speeds of the hub have been examined, giving the possibility to observe the dependence of performance characteristics on hub rotational speed. Increasing the rotational speed is found to improve the performance of the cascade by decreasing losses in the clearance region, while it affects the flow in the entire passage.

Nomenclature

C_x	=	blade axial chord
M	=	Mach number
M_u	=	hub peripheral Mach number
$\dot{m}$	=	mass flow rate
p_s	=	static pressure
p_t	=	total pressure
Q_{in}	=	dynamic inlet head at midspan, $p_t - p_s$
V	=	velocity
$\bar{\alpha}$	=	yaw angle relative to axial, $\tan^{-1}(\bar{V}_u/\bar{V}_x)$
θ	=	turning angle, Eq. (2)
$\bar{\omega}$	=	pressure loss coefficient, Eq. (1)

Subscripts and Superscripts

$\bar{Q}$ = circumferentially mass-averaged value of a quantity $Q(r, \phi)$ between angular positions ϕ_1 and ϕ_2

$$\bar{Q}(r) = \int_{\phi=\phi_1}^{\phi=\phi_2} Q(r,\phi)\cdot\frac{\mathrm{d}\dot{m}}{\Delta\dot{m}(r)} \quad \text{where}$$

$$\Delta\dot{m}(r) = \int_{\phi_1}^{\phi_2} \mathrm{d}\dot{m}$$

x, u, r	=	axial, circumferential, and radial component
1	=	upstream of the cascade
2	=	downstream of the cascade

Introduction

THE study of tip clearance effects has received considerable attention since the early days of turbomachine development. The presence of a blade tip clearance gap is the origin of losses, which may be of significant amount, while it influences the stability limit of compressors. Research efforts are continuing to the present day because the related phenomena are not yet fully understood.

Models for estimating the losses associated with clearance gaps have been proposed by several researchers. They can predict flow features with a degree of success that depends on the configurations examined, including the effect of the relative wall speed. In this respect, compressors and turbines need separate treatment. In compressors, the effect of viscous flow transport is in sympathy with the leakage flow due to blade surface pressure difference, whereas in turbines the effect is opposite. Reviews of methods for estimating tip clearance effects on compressor performance have been given by Lakshminarayana[1] and Peacock,[2] and Schmidt et al.[3] have examined applicability of existing correlations to data from a low-speed rotor. The development of a successful model requires a good physical knowledge of the phenomena and the parameters affecting them. That is why detailed tip clearance flowfield investigations are needed, and many of them have been performed in recent years into simple leakage rigs, cascades, or rotating machines.

Rains's[4] early experimental studies in a three-stage axial water pump and Dean's[5] studies in a low-speed linear compressor cascade with different gap heights and relative wall velocities have identified the presence of a leakage vortex and studied some of its features. Lakshminarayana and Horlock[6,7] investigated the features of the leakage vortex and its influence on static pressure distribution at the blade tip suction side, and they proposed a model for calculation of effects on cascade performance. They suggested an optimum gap-to-chord ratio for minimal flow separation at the blade tip region.

Water rigs with linear cascades were used by Gearhart[8] and Graham[9] to study the effect of wall relative movement on tip clearance flow, by using a moving belt. Gearhart[8] studied a compressor cascade and observed an increase of the mass flow rate through the clearance gap with the relative wall movement. Graham[9] studied a turbine cascade and produced pressure distributions at midspan and near the tip for different tip gaps and wall speeds.

A linear low-speed compressor cascade with different tip clearance gap sizes was used for a thorough flowfield investigation performed by Kang and Hirsch.[10,11] The measurement results manifested that the leakage vortex has a low total pressure quasi-circular core with high losses and a wakelike axial velocity profile, diffusing while moving downstream. During the tip clearance vortex evolution, its center moves away from both the blade suction surface and the endwall, and this motion induces a strong blade reloading that reinforces the leakage flow.

Morphis and Bindon[12] used an annular turbine cascade to examine the effect of relative wall motion on the pressure distribution of the blade tip. Yaras et al.[13,14] used a turbine cascade with a moving belt to study the flow inside the tip clearance and downstream of the blade row for varying relative wall velocities.

The flow in the tip region of a low-speed axial flow compressor rotor was measured by Murthy and Lakshminarayana.[15] The emergence of the leakage jet at approximately quarter chord and its eventual rollup resulted in the underturning of the flow at higher radii and overturning at lower radii. Further measurements of Lakshminarayana and Murthy[16] indicated the presence of a strong leakage vortex. Mixing between the wake and the leakage flow resulted in increased losses from the trailing edge to about half a

Received 30 March 2000; revision received 10 March 2001; accepted for publication 20 March 2001.

*Research Assistant, Laboratory of Thermal Turbomachines.
†Associate Professor, Laboratory of Thermal Turbomachines.
‡Professor, Laboratory of Thermal Turbomachines.

chord downstream. Subsequent work of Lakshminarayana et al.[17] on a low-speed axial compressor rotor showed that the leakage jet mixes quickly with the main through flow and was not seen to roll up into a vortex, a finding contrasting observations in low-speed cascades. Foley and Ivey[18] conducted a detailed investigation in a low-speed isolated compressor rotor. A vortex structure was identified and associated to the losses in the tip region.

Stauter[19] mapped the tip region flowfield in a two-stage, low-speed axial compressor. The measurements showed a continuous decay of the leakage vortex through the passage until aft of the trailing edge of the blades, at which point the radial flows started increasing again, reaching a peak at 115% chord, after which they started decreasing. Suder and Celestina[20] obtained some data from a high-speed compressor rotor with a limited coverage of the flowfield, namely, two circumferential planes near the tip wall, revealing a tip clearance flow structure similar to the one revealed by measurements produced from low-speed rigs.

Experimental study in a multistage compressor were performed by Foley[21] on a four-stage, low-speed axial compressor and two different tip clearance gap sizes. The measurements revealed that the fluid enters the blade row endwall regions with a high incidence, causing peak suction pressures to occur closer to the blade leading edge at the blade tip and root. At the blade tip, the peak suction pressure is maintained by the radial flow of fluid being entrained into the leakage jet. The decay of the leakage vortex is not complete at the exit to the blade row, and increased losses can become apparent in the root region downstream of the following blade row.

Information produced by detailed experimental studies has been used to build models for the study of clearance effects. For example, the work of Nikolos et al.,[20–25] incorporating a theoretical model for the influence of relative wall motion, gave the possibility to predict radial distributions of flow quantities, including losses, with good agreement with data from cascades and several compressor rotors.

Most of the experimental information, on which attempts for modelling tip clearance size effects have been based, comes from investigations in low-speed rigs. Nevertheless, it is not certain whether the same physical mechanisms still prevail inside high-speed flows, such as the flows in current gas turbine engines. The present investigation comes to provide, for the first time, data from a high-speed annular cascade with a clearance gap over a rotating hub wall, representative of realistic compressor operating conditions. It deals with cascade performance for varying relative wall velocity, using data from measurements at the inlet and outlet of the cascade. Three-dimensional flow structure, the effect of clearance gap size and the presence of wall rotation on the cascade performance, for two different gap sizes, have already been presented by Doukelis et al.[26,27]

Annular Cascade Configuration, Execution of Measurements

Facility

The layout of the annular cascade facility, as well as the principles for its design and construction, have been reported in detail by Mathioudakis et al.[28] An axial compressor, placed downstream, induces the flow in the test cascade. The airstream enters the facility via a smoothly contracting bellmouth into a scroll, which delivers the airflow with a swirl into a contracting axisymmetric bent duct, leading to the annular space with hub–tip ratio of 0.75. The test section, on which the test cascade is mounted follows, as can be seen in Fig. 1. The cascade has 19 untwisted blades of a chord of 100 mm, an aspect ratio of 0.8, maximum thickness-to-chord ratio of 4.58%, a solidity of 1.065 at midspan, and a 4% chord clearance gap size. The geometrical inlet and outlet angles of the blades are 60.1 and 44.6 deg from the axial direction, respectively (equivalent camber angle of 15.5 deg), whereas the stagger angle of the blades at midspan is 51.4 deg. The hub wall of the annular space can be rotated by a controlled speed electric motor, creating a relative motion between the endwall and the blade tip. The maximum local Mach number that can be achieved in the annulus at the cascade inlet is about 0.7, whereas the maximum peripheral Mach number of the hub wall is 0.51.

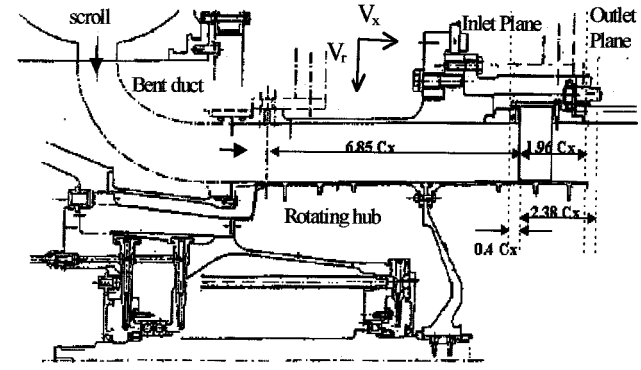

Fig. 1 Layout of the test section of the annular cascade facility.

Instrumentation and Measuring Locations

The objective of the present work is the study of the effect of the magnitude of the hub wall velocity relative to the blades on the performance of an annular compressor cascade. Measurements were conducted for this purpose by a conventional five-hole probe at the inlet and outlet of the cascade, at locations foreseen for this purpose. The maximum local Mach number in the annular space at the cascade inlet was about 0.6, giving a Reynolds number of approximately 1.1×10^6. Four different hub wall rotational speeds were examined, ranging from hub still to hub rotating at a peripheral Mach number $M_u = 0.504$.

At the cascade inlet (Fig. 1), radial traverses were performed at six circumferential locations, 0.4 axial chords upstream the leading edge of the blades. The six circumferential locations are fixed with respect to the blades and lie at different blade-to-blade positions. At the cascade outlet (Fig. 1), 11 radial traverses were conducted, 1.38 axial chords downstream the trailing edge of the blades. The probe was fixed on the casing, while the cascade was turned at different circumferential positions.

The short-stem, five-hole probe used for the current study has a stem diameter of 3 mm. The five-hole probe assembly was mounted on a remotely controlled traversing mechanism. The accuracy in setting the angular positioning of the cascade is ± 0.1 deg for a full rotation. The uncertainty of angle measurement for the alignment of the probe carriage, which is of the order of ± 0.3 deg, yields a systematic error to the measurement of the flow angles of the order of ± 0.3 deg. According to the calibration report of the probe (Schneider and Koschel[29]), the expected errors of the measured quantities are ± 0.1 deg for the yaw and pitch angles, $\pm 0.5\%$ for the total velocity, and $\pm 0.6\%$ for the total and static pressure.

Cascade Performance

The influence of the magnitude of the relative wall speed on the performance parameters of the cascade is now presented. First inlet and outlet flow distributions are discussed, followed by distributions of losses and turning.

Inlet and Outlet Conditions

Measurements at the annular cascade inlet and outlet were performed for each rotational speed under study. Figures 2 and 3 show the circumferentially mass-averaged profiles at the inlet and outlet of the cascade, for the four cases of hub rotation. Data from different circumferential locations at the exit of the connecting duct indicate that the total pressure gradient at the inlet midspan (Fig. 2c) has been produced at the scroll exit as a consequence of the shear layers generated inside the inlet bellmouth and the scroll. For flow paths exiting the scroll at its upper part (close to the scroll spiral centerline), where the flow has traveled a relatively small distance inside the scroll, a uniform total pressure profile is manifested around midspan at the corresponding circumferential locations at the scroll exit. The remaining circumferential locations, where the flow has traveled a much longer distance and the scroll cross section has become smaller, demonstrate a nonuniform total pressure profile all over the span.

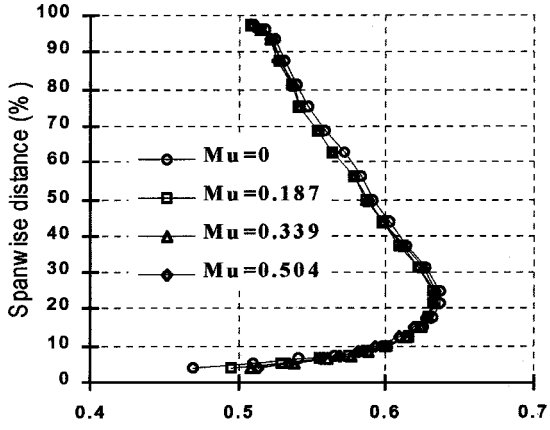

a) Mach number

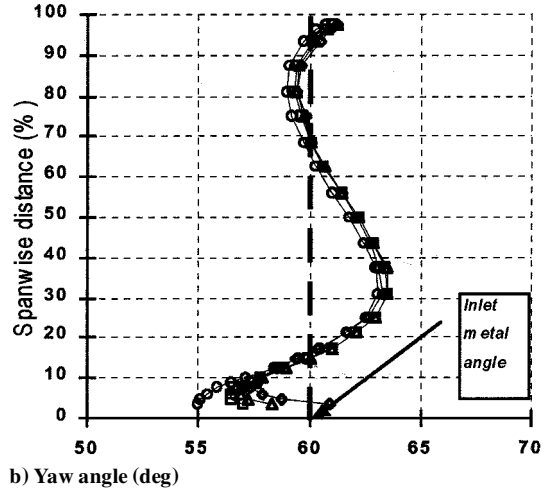

b) Yaw angle (deg)

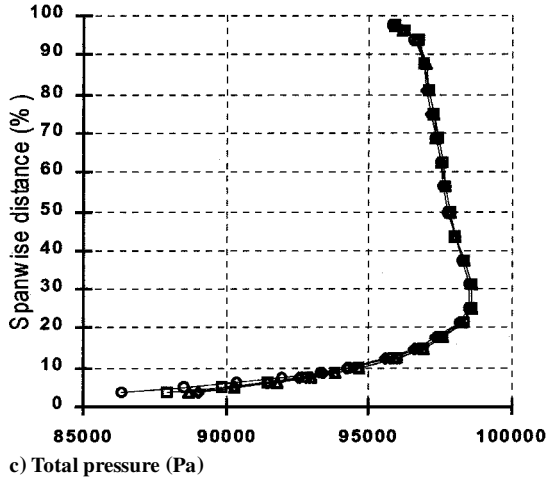

c) Total pressure (Pa)

Fig. 2 Flowfield properties at the cascade inlet.

The total pressure gradients close to the hub and casing closely resemble customary boundary layers. The inlet boundary layer is thicker in the hub region, covering the lower 25% of the span, whereas the boundary layer in the outer casing covers the upper 10% of the span, as shown in Fig. 2c. The hub wall rotation influence is felt mainly in the lower 15% of the span, inside the hub boundary layer. The total pressure profile at the inlet and outlet of the cascade is less steep near the wall as the rotational speed is increased, leading to a higher total pressure near the hub because of the increased energy transfer from the moving wall to the fluid.

The yaw angle is also influenced by variation in the relative wall speed. An increase in hub rotational speed entrains the fluid near the wall and changes the flow angle profile, as shown in Fig. 2b. As one would expect, near the wall, the angle increases, and it would be expected to arrive to a value of 90 deg on the wall. This behavior has a significant consequence on the operation of the cascade. While with the hub wall stationary the blade operates at a maximum local incidence of about 5 deg, as the rotational speed is increased, the incidence decreases by as much as 2.5 deg in the lower 10% of the blade span, for the higher rotational speed. Finally, Mach number is also influenced, showing larger values in the vicinity of the hub wall, as the relative wall velocity is increased.

The distributions of flow quantities at the upstream location were independent of the size of the clearance gap. Circumferential nonuniformity was found to be very small on a blade passage scale.[27]

The following remarks can be made on the cascade outlet flow properties (Fig. 3):

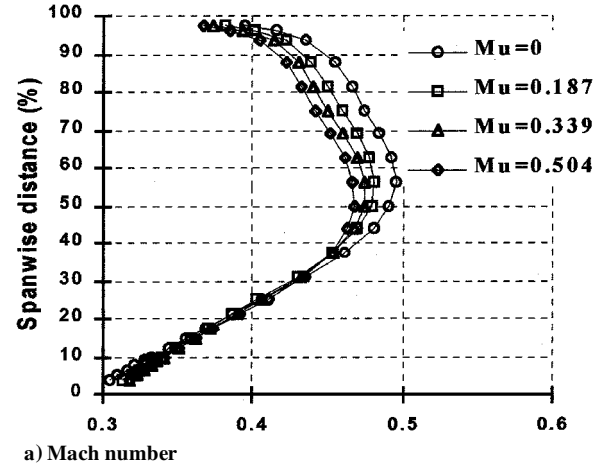

a) Mach number

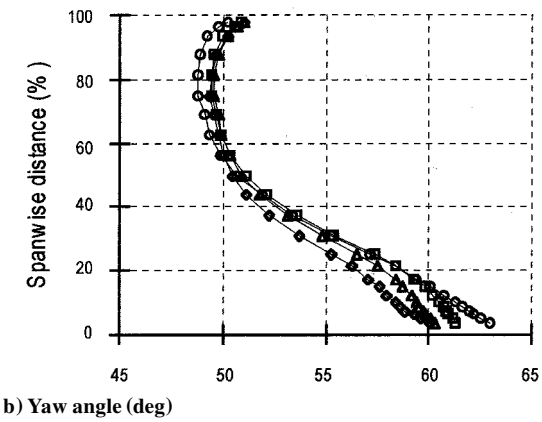

b) Yaw angle (deg)

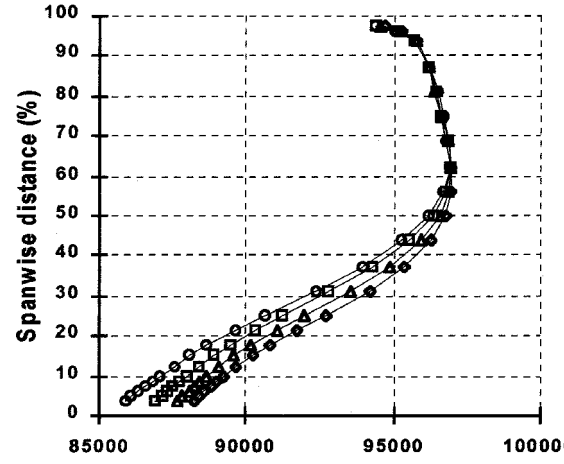

c) Total pressure (Pa)

Fig. 3 Flowfield properties at the cascade outlet.

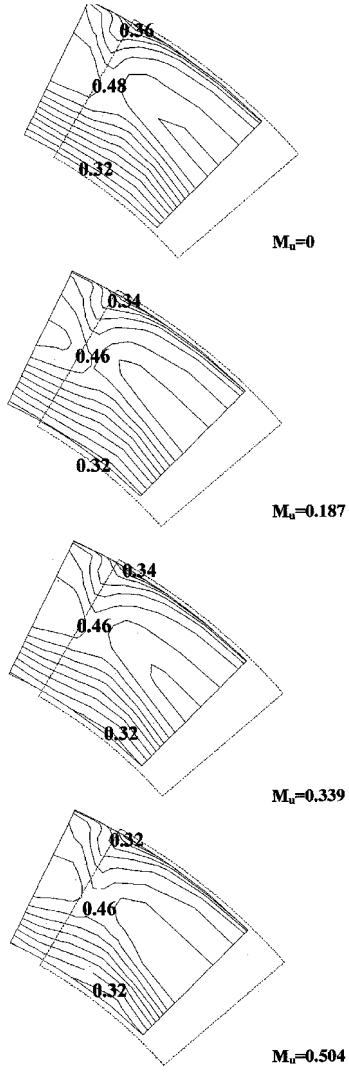

Fig. 4 Mach number distributions at the cascade outlet (step = 0.02).

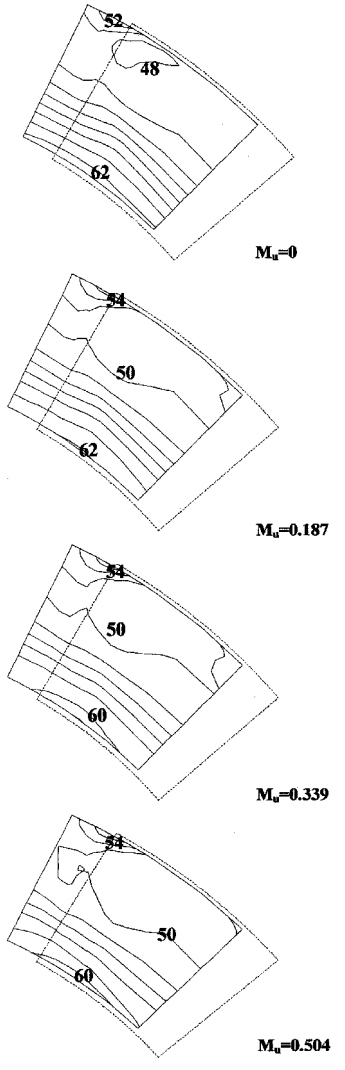

Fig. 5 Yaw angle distributions at the cascade outlet (step = 2 deg).

1) The hub viscous layer is significantly thicker than upstream, extending up to 50% blade span, and is thicker for low wall relative velocities.

2) For all of the quantities, the gradients in the hub region are steeper for lower rotational speeds.

3) The changes in the hub viscous layer clearly influence the remaining upper part of the passage. For this part, the blockage effect results in higher Mach numbers in low rotational speeds.

4) The tip viscous layer does not seem to have been significantly influenced by the development of the hub layer, in any case.

The distributions of Mach number and yaw angle at the cascade outlet over an area corresponding to one blade passage are shown in Figs. 4 and 5. The dashed outline represents the passage projection along the trailing-edge metal angle of the blades. An area of low Mach numbers covers the region near the hub wall, indicating a thick boundary layer at this location. The radial extent of this area is larger for the stationary hub, and it grows thinner as the hub rotational speed is increased. An area of low values, corresponding apparently to the blade wake, extends through the upper part of the span. The wake still persists at 1.38 axial chords downstream, while it is skewed because of the radial variation of flow angle. Distributions of flow angle (Fig. 5) show that there are small circumferential variations, whereas significant radial variations with higher angle values near the hub are observed for the lower rotational speeds.

Finally, Fig. 6 shows that blade loading is influenced by wall rotation: static pressure distributions at two spanwise locations, one close to the clearance gap (7.5% of span from hub) and one at a farther radial position (78.8% of span), as well as on the blade tip

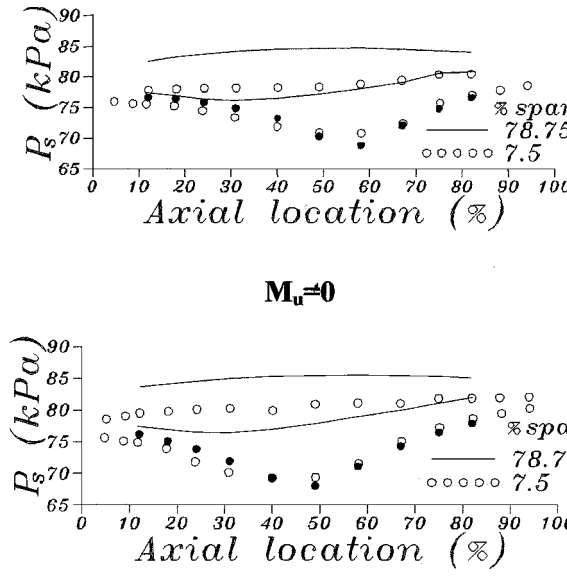

Fig. 6 Static pressure distribution on blade surface: •, pressure inside the gap.

centerline, inside the clearance gap itself. The effect of hub wall rotation acts in the same direction as the leakage flow for a compressor cascade. It is, therefore, expected that hub rotation will strengthen the vortex and displace the position of minimum static pressure upstream, as well as produce a larger perturbation on the blade surface static pressure distribution. This is clearly demonstrated from Fig. 6 for pressure distribution inside the gap and at the radial location in the gap vicinity. The position of minimum static pressure moves from approximately 59% of the chord for the stationary case to 50% for the rotating case.

Cascade Performance Parameters

We will now examine the performance of the cascade for different relative hub wall speeds. The cascade performance is examined through the loss coefficient $\bar{\omega}$ and the turning angle θ, which are defined as follows:

$$\bar{\omega} = \frac{\overline{p_{t1}} - \overline{p_{t2}}}{\overline{p_{t1}} - \overline{p_{s1}}} \tag{1}$$

$$\theta = \bar{\alpha}_1 - \bar{\alpha}_2 \tag{2}$$

In Eqs. (1) and (2), subscripts 1 and 2 denote the upstream and downstream quantities at the same radius. These parameters are derived by circumferentially mass averaging the measured distributions of flowfield properties. Although the use of an alternative pressure loss coefficient, based on the streamlines, would be desirable in view of the three dimensionality of the flow under study, this would be possible only if detailed enough data for the flow within the passage were available.

Figure 7 shows the pressure loss coefficient for all cases of relative wall speed. The loss distributions indicate a region of high losses in the lower-half of the passage, which is the clearance influence region. Lower values, with no significant variation are observed in the upper-half, with a local increase near the tip endwall. The magnitude of the losses is significantly larger for lower rotational speeds, a difference that can be attributed to two factors: 1) that rotation of the hub wall energizes the boundary layer, transferring energy to the flow, with a beneficial effect on both the inlet viscous layer and its subsequent development through the passage, and 2) that, in the lower relative wall velocities, the hub section of the blade operates at higher incidence angles, favoring the rapid development of both endwall and blade boundary layers and resulting in a thicker shear layer at the exit of the cascade. Note that the form of the loss coefficient distribution observed here for the clearance region is the typical one obtained by other experiments as well as theoretical analysis of tip clearance losses.[24]

Performance of the cascade in terms of turning angle can be seen in Fig. 8. It is observed that the turning angle remains approximately constant in the upper-half of the span, while it is increased

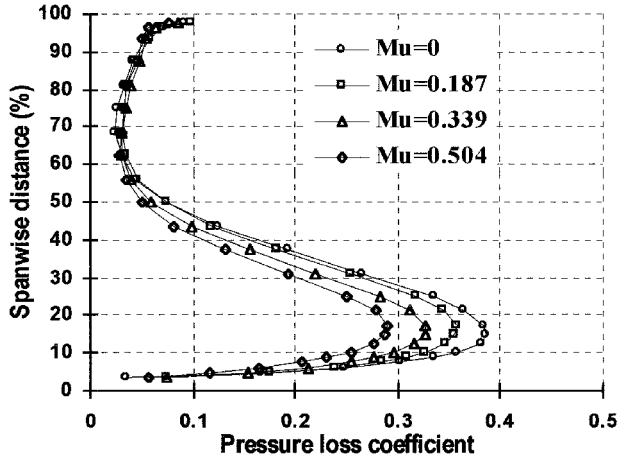

Fig. 7 Spanwise distribution of circumferentially mass-averaged pressure loss coefficient for varying hub rotational speed.

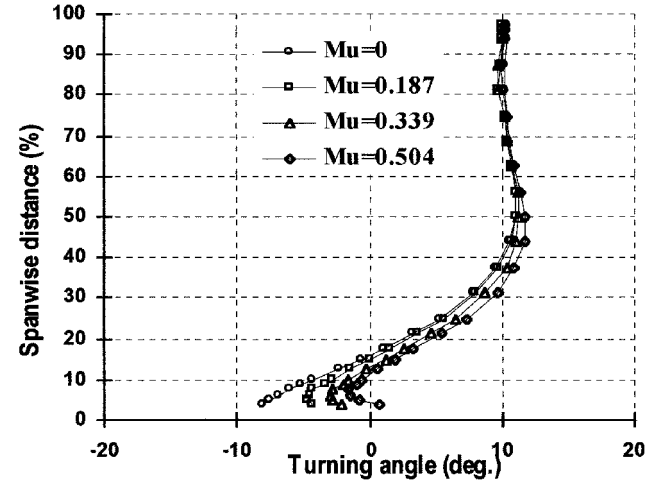

Fig. 8 Spanwise distribution of circumferentially mass-averaged pressure turning angle for varying hub rotational speed.

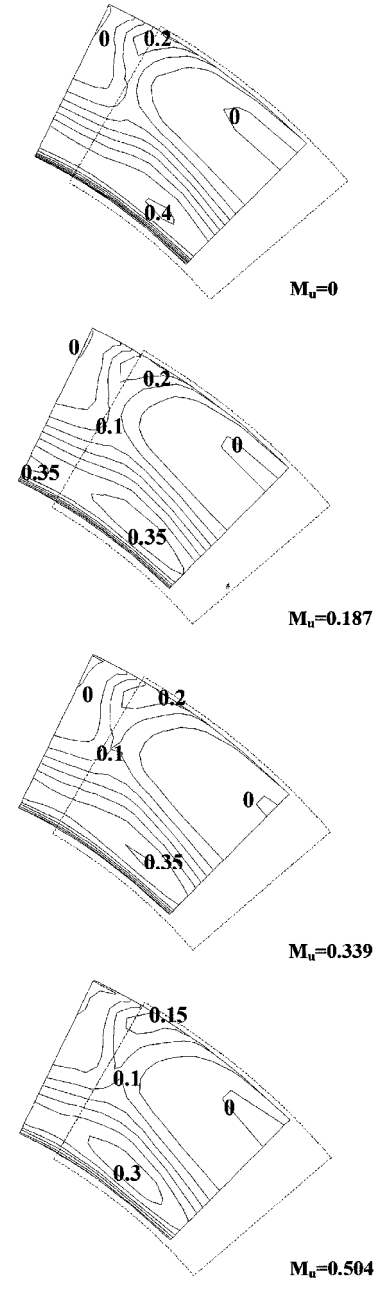

Fig. 9 Pressure loss coefficient distributions (step = 0.05).

significantly in the lower one, as the hub rotational speed is increased. The lower 10% even exhibits negative turning angles for the lower rotational speeds, indicating significant viscous action in the passage, which must have included some form of three-dimensional separation.

An additional insight on the features of the flow related to the preceding observations can be gained from observation of Fig. 9, where the distribution of loss coefficient at the outlet of the cascade, over an area corresponding to one passage, is shown. The isocontours show islands of high loss, attributed to the presence of a leakage vortex, not mixed out yet at this axial location. The size of this island, for loss above a certain level, is consistently becoming smaller as the hub rotational speed is increased, being consistent with the observations derived from the mass-averaged distributions.

The variation of the overall pressure loss coefficient of the cascade and the maximum loss coefficient (occurring at about 13% height from the hub) is presented in Fig. 10. The overall pressure loss coefficient is calculated by integration of the pressure loss coefficient distributions in the circumferential and radial direction, whereas the maximum loss coefficient is the pressure loss coefficient at the radial location where it exhibits the maximum value. It is observed that, although at small rotational speeds the overall loss does not seem to be influenced by the rotation of the hub, further increase leads to overall loss coefficient reduction. The loss coefficient, on the other hand, is continuously decreasing with hub speed. This behavior reflects the change of loss coefficient distribution over the height, shown in Fig. 7. The reduction of the local values as the speed increases is compensated for by a small increase at the upper-half of the span, which does not happen as the speed increases further.

Finally, the variation of turning angle within the wall influence region is presented in Fig. 11. It is shown that the turning performance is enhanced as the rotational speed increases, and the influence becomes less pronounced as we move farther from the wall.

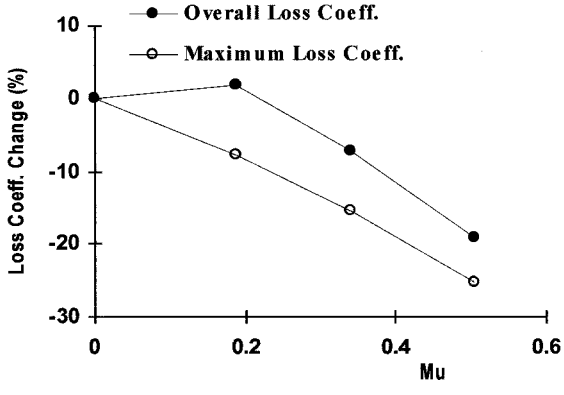

Fig. 10 Overall and maximum total pressure loss coefficient variation, as function of the hub speed.

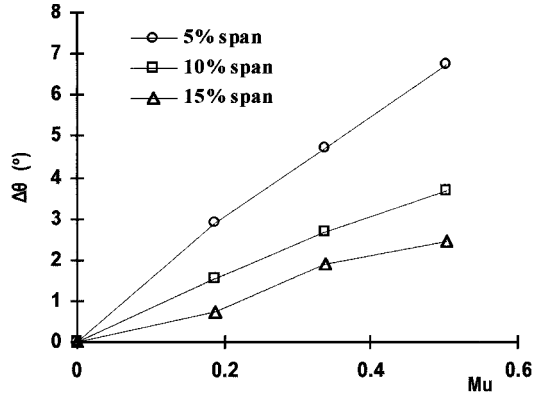

Fig. 11 Turning angle variation (difference from value when hub is still), as function of the hub speed, for different spanwise locations.

Conclusions

In the present work, an experimental investigation of the influence of the magnitude of the relative wall speed on the performance of a high-speed annular compressor cascade with hub clearance has been conducted. Five-hole probe measurements, conducted at the inlet and outlet of the cascade for four different rotational speeds of the hub, have been used to derive blade performance characteristics in the form of loss and turning distributions. Increasing the hub rotational speed was found to improve the performance of the cascade by decreasing losses in the clearance region and creating a more favorable operating condition than the stationary wall case, while it affects the flow in the entire passage. The favorable operating conditions are attributed to the changes of local incidence as a result of entrainment and energy transfer from the hub wall to the boundary layer.

References

[1]Lakshminarayana, B., "Compressor Loss Correlations, Experimental Investigation on the Effects of Tip Clearance in Turbomachinery," Von Kármán Inst. Lecture Series 1985-05, Brussels, 1985.

[2]Peacock, R. E., "Turbomachinery Tip Gap Aerodynamics—A Review," *Proceedings of the 9th International Symposium on Air Breathing Engines*, Athens, 1989, pp. 549–558.

[3]Schmidt, M. J. P., Agnew, B., and Elder, R. L., "Tip Clearance Flows—Part 1, Experimental Investigation of an Isolated Rotor," *Proceedings of the 8th International Symposium on Air Breathing Engines*, Cincinnati, 1987, pp. 291–297.

[4]Rains, D. A., "Tip Clearance Flows in Axial Compressors and Pumps," Ph.D. Dissertation, Hydrodynamics and Mechanical Engineering Labs., California Inst. of Technology, Pasadena, CA, 1954.

[5]Dean, R. C., "The Influence of Tip Clearance on Boundary Layer Flow in a Rectilinear Cascade," Gas Turbine Lab., Rept. 27-3, Massachusetts Inst. of Technology, Cambridge, MA, Dec. 1954.

[6]Lakshminarayana, B., and Horlock, J. H., "Tip Clearance Flow and Losses for an Isolated Compressor Blade," Aeronautical Research Council, ARC R&M 3316, 1962.

[7]Lakshminarayana, B., and Horlock, J. H., "Leakage and Secondary Flows in Compressor Cascades," Aeronautical Research Council, ARC R&M 3483, March 1965.

[8]Gearhart, W. S., "Tip Clearance Cavitation in Shrouded Underwater Propulsors," *Journal of Aircraft*, Vol. 3, No. 2, 1966.

[9]Graham, J. A. H., "Investigation of a Tip Clearance Cascade in a Water Analogy Rig," American Society of Mechanical Engineers, ASME Paper 85-IGT-65, 1985.

[10]Kang, S., and Hirsch, C., "Experimental Study of the Three Dimensional Flow Within a Compressor Cascade with Tip Clearance. Part I: Velocity and Pressure Fields," American Society of Mechanical Engineers, ASME Paper 92-GT-215, 1992.

[11]Kang, S., and Hirsch, C., "Experimental Study of the Three Dimensional Flow Within a Compressor Cascade with Tip Clearance. Part II: The Tip Leakage Vortex," American Society of Mechanical Engineers, ASME Paper 92-GT-432, 1992.

[12]Morphis, G., and Bindon, J. P., "The Effects of Relative Motion, Blade Edge Radius and Gap Size on the Blade Tip Pressure Distribution in an Annular Turbine Cascade with Clearance," American Society of Mechanical Engineers, ASME Paper 88-GT-256, 1988.

[13]Yaras, M. I., Sjolander, S. A., and Kind, R. J., "Effects of Simulated Rotation on Tip Leakage in a Planar Cascade of Turbine Blades. Part I: Tip Gap Flow," ASME Paper 91-GT-127, 1991.

[14]Yaras, M. I., Sjolander, S. A., and Kind, R. J., "Effects of Simulated Rotation on Tip Leakage in a Planar Cascade of Turbine Blades. Part II: Downstream Flow Field and Blade Loading," American Society of Mechanical Engineers, ASME Paper 91-GT-128, 1991.

[15]Murthy, K. N. S., and Lakshminarayana, B., "Laser Doppler Velocimeter Measurement in the Tip Region of a Compressor Rotor," *AIAA Journal*, Vol. 24, No. 5, 1986, pp. 807–814.

[16]Lakshminarayana, B., and Murthy, K. N. S., "Laser Doppler Velocimeter Measurement of Annulus Wall Boundary Layer Development in a Compressor Rotor," American Society of Mechanical Engineers, ASME Paper 87-GT-251, May–June 1987.

[17]Lakshminarayana, B., Zaccaria, M., and Marathe, B., "The Structure of Tip Clearance Flow in Axial Flow Compressors," *Journal of Turbomachinery*, Vol. 117, July 1995, pp. 336–346.

[18]Foley, A. C., and Ivey, P. C., "3D Laser Transit Measurements of the Tip Clearance Vortex in a Compressor Rotor Blade Row," American Society of Mechanical Engineers, ASME Paper 96-GT-506, 1996.

[19]Stauter, R. C., "Measurement of the Three-Dimensional Tip Region Flowfield in an Axial Compressor," American Society of Mechanical

Engineers, ASME Paper 92-GT-211, 1992.

[20]Suder, K. L., and Celestina, M. L., "Experimental and Computational Investigation of the Tip Clearance Flow in a Transonic Axial Compressor Rotor," American Society of Mechanical Engineers, ASME Paper 94-GT-365, 1994.

[21]Foley, A. C., "Tip Clearance Effects in Low Speed Axial Flow Compressors," Ph.D. Thesis, School of Mechanical Engineering, Cranfield Univ., Cranfield, England, U.K., Jan. 1995.

[22]Nikolos, J., Douvikas, D., and Papailiou, K., "A Method for the Calculation of the Tip Clearance Flow Effects in Axial Flow Compressors. Part I: Description of Basic Models," American Society of Mechanical Engineers, ASME Paper 93-GT-150, 1993.

[23]Nikolos, J., Douvikas, D., and Papailiou, K., "A Method for the Calculation of the Tip Clearance Flow Effects in Axial Flow Compressors. Part II: Calculation Procedure," American Society of Mechanical Engineers, ASME Paper 93-Gt-151, 1993.

[24]Nikolos, J., Douvikas, D., and Papailiou, K., "Theoretical Modelling of Relative Wall Motion Effects in Tip Leakage Flow," American Society of Mechanical Engineers, ASME Paper 95-GT-88, 1995.

[25]Nikolos, J., Douvikas, D., and Papailiou, K., "Modelling of the Tip Clearance Losses in Axial Flow Machines," American Society of Mechanical Engineers, ASME Paper 96-GT-72, 1996.

[26]Doukelis, A., Mathioudakis, K., and Papailiou, K., "The Effect of Tip Clearance Size and Wall Rotation on the Performance of a High-Speed Annular Compressor Cascade," American Society of Mechanical Engineers, ASME Paper 98-GT-38, 1998.

[27]Doukelis, A., Mathioudakis, K., and Papailiou, K., "Investigation of the 3-D Flow Structure in a High-Speed Annular Compressor Cascade for Tip Clearance Effects," American Society of Mechanical Engineers, ASME Paper 98-GT-39, 1998.

[28]Mathioudakis, K., Papailiou, K., Neris, Bonhommet, C., Albrand, G., and Wenger, U., "An Annular Cascade Facility for Studying Tip Clearance Effects in High Speed Flows," *Proceedings of the XIII International Symposium for Air Breathing Engines*, Chattanooga, TN, Sept. 1997, pp. 831–839.

[29]Schneider, A., and Koschel, W., "Five Hole Pressure Probe 955-01, no. 1, Calibration Report," Inst. für Strahlantriebe und Turboarbeitsmaschinen, Rheinisch-Westfälische Technische Hochschule, Aachen, Germany, 1994.